



**HAL**  
open science

## Effects on CHP plant efficiency of H<sub>2</sub> production through partial oxydation of natural gas over two group VIII metal catalysts

Olivier Le Corre, Khalil Saikaly, Marc A. Rosen

► **To cite this version:**

Olivier Le Corre, Khalil Saikaly, Marc A. Rosen. Effects on CHP plant efficiency of H<sub>2</sub> production through partial oxydation of natural gas over two group VIII metal catalysts. *International Journal of Hydrogen Energy*, 2012, 37 (13), pp.10380-10389. 10.1016/j.ijhydene.2012.04.015 . hal-00841027

**HAL Id: hal-00841027**

**<https://hal.science/hal-00841027>**

Submitted on 22 Jul 2013

**HAL** is a multi-disciplinary open access archive for the deposit and dissemination of scientific research documents, whether they are published or not. The documents may come from teaching and research institutions in France or abroad, or from public or private research centers.

L'archive ouverte pluridisciplinaire **HAL**, est destinée au dépôt et à la diffusion de documents scientifiques de niveau recherche, publiés ou non, émanant des établissements d'enseignement et de recherche français ou étrangers, des laboratoires publics ou privés.

**EFFECTS ON CHP PLANT EFFICIENCY OF H<sub>2</sub> PRODUCTION  
THROUGH PARTIAL OXYDATION OF NATURAL GAS OVER TWO GROUP VIII METAL  
CATALYSTS**

O. Le Corre<sup>1</sup>, K. Saikaly<sup>2</sup> and M. A. Rosen<sup>3</sup>

<sup>1</sup> GEPEA – Ecole des Mines de Nantes – CNRS - UMR 6144, 4 rue A. Kastler – BP 20722 – F 44307  
Nantes, France

<sup>2</sup> CREED, Research center of VEOLIA Environment, 291 av D. Dreyfus, 78520 Limay, France

<sup>3</sup> Faculty of Engineering and Applied Science, University of Ontario Institute of Technology, Oshawa, Ontario,  
L1H 7K4, Canada

Corresponding author: [lecorre@emn.fr](mailto:lecorre@emn.fr)

Phone : (+33) 2 51 85 82 57

Fax : (+33) 2 51 85 82 99

## 1 ABSTRACT

2  
3 Blending H<sub>2</sub> with natural gas in spark ignition engines can increase for electric efficiency. In-situ H<sub>2</sub>  
4 production for spark ignition engines fuelled by natural gas has therefore been investigated recently, and  
5 reformed exhaust gas recirculation (RGR) has been identified a potentially advantageous approach: RGR  
6 uses the steam and O<sub>2</sub> contained in exhaust gases under lean combustion, for reforming natural gas and  
7 producing H<sub>2</sub>, CO, and CO<sub>2</sub>. In this paper, an alternative approach is introduced: air gas reforming circulation  
8 (AGRC). AGRC uses directly the O<sub>2</sub> contained in air, rendering the chemical pathway comparable to partial  
9 oxidation. Formulations based on palladium and platinum have been selected as potential catalysts. With  
10 AGRC, the concentrations of the constituents of the reformed gas are approximately 25% hydrogen, 10%  
11 carbon monoxide, 8% unconverted hydrocarbons and 55% nitrogen. Experimental results are presented for  
12 the electric efficiency and exhaust gas (CO and HC) composition of the overall system (SI engine equipped  
13 with AGRC). It is demonstrated that the electric efficiency can increase for specific ratios of air to natural gas  
14 over the catalyst. Although the electric efficiency gain with AGRC is modest at around 0.2%, AGRC can be  
15 cost effective because of its straightforward and inexpensive implementation. Misfiring and knock were both  
16 not observed in the tests reported here. Nevertheless, technical means of avoiding knock are described by  
17 adjusting the main flow of natural gas and the additional flow of AGRC.

18  
19 **Keywords:** Hydrogen, CHP, natural gas, power,

## 20 21 1. INTRODUCTION

22  
23 Efforts to improve the performance of internal combustion (IC) engines (e.g., brake mean effective pressure,  
24 specific fuel consumption) are nowadays limited by both stringent emissions regulations and abnormal  
25 combustion problems (knock, engine misfiring). These limitations are particularly important for lean burn natural  
26 gas engines that are used for combined heat and power (CHP) applications. Examples of such constraints are  
27 shown in Figure 1, where engine performance parameters are plotted against equivalence ratio. Improving the  
28 electric efficiency of stationary IC engines fuelled by natural gas should not cause any of the above noted  
29 constraints to be exceeded. The window between knock and combustion misfire is narrow, as shown in the left  
30 diagram of Figure 1, and can occur for an equivalence ratio in the range 1.7 to 2.0, common tuning for CHP  
31 applications. Nevertheless, specific emissions are relatively low in this equivalence ratio range, as shown in the  
32 right diagram of Figure 1, suggesting that a good compromise among these factors is attained by operating in  
33 this equivalence ratio range.

34  
35 Fig. 1. Variation of selected engine performance parameters with equivalence ratio, highlighting challenges  
36 (firing problems, emissions) in improving engine performance

37  
38 It has been demonstrated experimentally by Le Corre et al. [1] that the addition of H<sub>2</sub> has a positive effect on IC  
39 engines fuelled by traditional fuels. Increased H<sub>2</sub> content increases the mechanical efficiency of such IC

40 engines without major increases in engine emissions. The main hindrance related to this measure is the  
41 requirement for H<sub>2</sub> storage cylinders, especially for transport applications.

42

43 To comply with emissions regulation two main approaches exist according to Einewall et al. [2]: operating under  
44 stoichiometric conditions with exhaust gas recirculation and a three-way catalyst, or operating under lean burn  
45 conditions.

46

47 In-situ H<sub>2</sub> production by steam reforming has been considered for IC engines fuelled by natural gas (e.g., Yap et  
48 al. [3]). Such applications are suitable for stationary CHP plants which are not subject to significant weight and  
49 volume constraints. In-situ steam reforming involves the following:

50

- 51 1. The catalytic reforming device is located in the exhaust gases in order to keep it at high  
52 temperature (775 K).
- 53 2. Part of the exhaust gases is used to supply the catalyst with water vapour, oxygen and carbon  
54 dioxide,
- 55 3. Reformed gases (enriched in hydrogen) are then mixed with the intake air and gas line, as is  
56 done with exhaust gas recirculation (EGR) technology used in the car industry to reduce NO<sub>x</sub>  
57 emissions for diesel engines.

58

59 Le Corre et al. [1] highlighted the effect of air-fuel ratio on the H<sub>2</sub> production for a CHP plant. The higher the air-  
60 fuel ratio, the greater is the H<sub>2</sub> content in the reformed gases. For example, Le Corre et al. [1] reported that the  
61 difference of H<sub>2</sub> content is 2% for air-fuel ratios of 1.5 and 1.4. This observation implies that the O<sub>2</sub> content limits  
62 reactions where it is a reactant. Two such reactions are the complete oxidation of methane and the partial  
63 oxidation of methane:

64

65 Complete oxidation of methane:  $\text{CH}_4 + 2\text{O}_2 \rightarrow \text{CO}_2 + 2\text{H}_2\text{O}$  ( $\Delta H_{298\text{ K}} = -890 \text{ kJ mol}^{-1}$ ) (1)

66 Partial oxidation of methane:  $\text{CH}_4 + \frac{1}{2}\text{O}_2 \rightarrow \text{CO} + 2\text{H}_2$  ( $\Delta H_{298\text{ K}} = -35.6 \text{ kJ mol}^{-1}$ ) (2)

67

68 The individual reactions that contribute to the overall reaction consist of the reforming of CO<sub>2</sub> into CO  
69 (equation 3), the steam reforming of methane into CO (equation 4), the water gas shift reaction (equation 5),  
70 the oxidation of hydrogen (equation 6) and the oxidation of carbon monoxide (equation 7):

71

72  $\text{CH}_4 + \text{CO}_2 \rightarrow 2\text{CO} + 2\text{H}_2$  (3)

73  $\text{CH}_4 + \text{H}_2\text{O} \rightarrow \text{CO} + 3\text{H}_2$  (4)

74  $\text{CO} + \text{H}_2\text{O} \rightarrow \text{CO}_2 + \text{H}_2$  (5)

75  $2\text{H}_2 + \text{O}_2 \rightarrow 2\text{H}_2\text{O}$  (6)

76  $2\text{CO} + \text{O}_2 \rightarrow 2\text{CO}_2$  (7)

77

78 For a CHP plant fuelled by natural gas, the O<sub>2</sub> content in the exhaust gases is around 7-8% by vol. In this  
79 configuration for H<sub>2</sub> production, hydrogen makes up around 10-14% by vol. of dry reformed gases. Then, O<sub>2</sub>  
80 content should be an important reactant.

81

82 Note that the exhaust gases from natural gas CHP plant typically contain three times less than the O<sub>2</sub>  
83 concentration in the air. This circumstance raises a question: Could the system be modified in a way that allows  
84 the exhaust gases to be substituted for some of the additional air provided at the reformer inlet?

85

86 The partial oxidation of methane has many advantages compared to steam reforming of methane for hydrogen  
87 production. An exothermic reaction, the partial oxidation of methane produces syngas with a H<sub>2</sub>/CO volumetric  
88 ratio of about two, which is ideal for further methanol and Fischer-Tropsch syntheses, according to Hadj-Sadok  
89 Ouaguenouni et al. [4]. Many precious metals, such as Ru, Rh and Pt, have been tested as catalysts for the  
90 partial oxidation of methane reaction (see Torniainen et al. [5]; Schmidt and Huff [6]). Schmidt et al. [7] and  
91 Deutschmann and Schmidt [8] have proposed a model to understand the complex interaction between transport  
92 and kinetics involved in the partial oxidation of methane. Some authors have tested a commercial nickel-based  
93 catalyst, but this approach was rejected due to activation difficulties. Pd and Pt have been identified as  
94 advantageous potential catalysts, and are considered here.

95

96 The main objective of this paper are to investigate the use of partial oxidation of methane as a means of  
97 improving H<sub>2</sub> production in CHP plant applications, and to examine how the process occurs in the presence of  
98 two group VIII metal catalysts (Pt and Pd). It is recognized that this approach must be cost effective for it to be  
99 adopted in real applications.

100

101 The concept considered here, which is referred to as air gas reforming circulation (AGRC), is shown in  
102 Figure 2. A catalytic reforming device is placed in the exhaust gas flow, but the catalysts do not come into  
103 contact with the exhaust gas, as it is used only to heat the catalyst. A chemically active blend of air and  
104 natural gas is located over the catalyst. The reformed gases are then mixed with the fresh mixture of fuel  
105 and air at the engine inlet. The results are reported in this paper of experimental studies in which two DCL©  
106 catalysts are examined: one based on Pt and one on Pd.

107

108

109 *Legend: (10) air flow meter, (11) air filter, (12) carburetor, (13) turbocharger, (14) intercooler, (15) actuator,*  
110 *(16) engine, (17) catalyst device, (18) exhaust heat exchanger, (20) natural gas flow meter, (21) Methane*  
111 *Number sensor, (30) additional air flow meter, (40) additional natural gas flow meter, (50) methane number*  
112 *sensor.*

113

114 Fig. 2. Engine system incorporating the air gas reforming circulation (AGRC) concept.

115

## 116 **2. EXPERIMENTAL APPARATUS AND PROCEDURE**

117

118 The test bench is a spark ignition (SI) engine fuelled by natural gas (see Figure 3). This installation is a  
119 combined heat and power plant operating at a fixed engine speed, as specified in Table 1.

120

121 Table 1. Engine specifications.

122

Fig. 3. Reforming device installation (at left) on a 210 kW<sub>e</sub> CHP gas engine (orange).

The engine generates a constant electrical power of 210 kW during operation. This power output is kept constant by a control loop that acts on a butterfly valve which adjusts the air-gas flow entering the cylinders. The air-fuel ratio is controlled manually by acting on the output of pressure reducer upstream of the carburetor using the Venturi effect [9]. The engine spark advance is kept constant throughout the testing, at 14 CA BTDC.

The test bench is equipped with various experimental sensors, corresponding to low frequency measurements (1 Hz). Measurement ranges are shown in parentheses.

- Thermocouples to measure the catalyst inlet and outlet temperature, and exhaust gas inlet and outlet temperature in the catalyst housing.
- A mass flow rate meter for the main natural gas SI engine feed line (0-1200 Nm<sup>3</sup>/h), and a mass flow rate meter for the additional natural gas at the catalyst inlet (0-600 Nm<sup>3</sup>/h).
- A mass flow rate meter for the intake air (0-1500 kg/h).
- Two dry-basis gas analysers:
  - Engine exhaust gases are analysed with the following:
    - HORIBA VA300 analyser: O<sub>2</sub> (0-25%), CO<sub>2</sub> (0-20%) CO (0-1%), NO (0-2000 ppm)
    - COSMA Cristal 500 analyser: HC (0-5000 ppm)
  - Catalyst outlet gases are analysed with the following:
    - ROSEMOUNT NGA2000: H<sub>2</sub> (0-30%), O<sub>2</sub> (0-30%), CH<sub>4</sub> (0-30%), CO (0-30%), CO<sub>2</sub> (0-30%)
    - SIEMENS H3-600: CO<sub>2</sub> (0-16%)
- A wattmeter (ENERNIUM-CFG1).
- A mass flow rate meter for the water cooling flow rate of SI engine (0-50 m<sup>3</sup>/h).
- PT sensors to measure the temperatures at several points in water cooling circuit of the engine (PT100, 0-200 °C).

All data were averaged over a period of 15 minutes once steady state operation was achieved. The H<sub>2</sub>-enhanced engine electrical efficiency  $\eta_e$  is defined as follows:

$$\eta_e = \frac{W_e}{LHV (q_{NG} + q_{NGR})} \quad (8)$$

Here,  $q_{NG}$  denotes the natural gas flow rate (main stream),  $q_{NGR}$  the natural gas flow rate for reforming, and  $LHV$  the lower heating value of natural gas. The two natural gas flows are shown in Figure 2.

The catalytic reforming device is illustrated in Figure 4.

The following experimental procedure was used for the catalytic reforming device shown in Figure 4:

163  
164  
165  
166  
167  
168  
169  
170  
171  
172  
173  
174  
175  
176  
177  
178  
179  
180  
181  
182  
183  
184  
185  
186  
187  
188  
189  
190  
191  
192  
193  
194  
195  
196  
197  
198  
199  
200  
201  
202  
203

1. The additional air flow rate over the catalytic reforming device was set.
2. The additional natural gas flow rate at catalyst inlet was set. Consequently, part of natural gas is not converted; this is not a disadvantage of the system since the main natural gas flow rate is decreased correspondingly.
3. The equivalence ratio of the SI engine is kept constant by modifying the air flow rate in the main stream. Note that the  $O_2$  content in the exhaust line is measured, and provides a straightforward means of maintaining the same condition during the combustion phase.

Fig. 4. Schematic of catalytic device. UHC denotes unburned hydrocarbons.

Two commercial honey-comb catalysts of DCL© are tested. These are made of formulations based on Pd and Pt, which are proprietary information of DCL©. Selected features of the catalysts are listed in Table 2.

Table 2. Features of tested catalysts

For safety reasons, the following measures were adopted:

- The system is operated at 80% of its nominal electric power output. This engine operation is less demanding than operation with a full fuel charge.
- Some part of additional natural gas flow rate over catalyst does not react. That is, oxygen is completely consumed at the catalyst outlet. This operational condition for the catalyst is safer since it permits auto-ignition of  $H_2$  to be avoided.

The volumetric flow rate over the honey-comb catalyst is a blend of additional air and natural gas for reforming, denoted NGR. Two flow rates for “additional air” are used: 3 and 5  $Nm^3/h$ . The range of the volumetric ratio  $NGR/O_2$  is bounded between 0.3 and 1.6, regardless of the catalyst, as shown in Figure 5. This volumetric ratio represents the ratio of the volumetric flow rate of natural gas for reforming to the volumetric flow rate of oxygen, in the overall gas flow. It is noted that, in the literature on steam reforming of natural gas, results are typically based on the ratio  $NGR/H_2O$  (e.g., Peucheret et al. [10]). Nonetheless, in this paper, the significant ratio is  $NGR/O_2$ .

Fig. 5. Experimental design of flow rates of additional air over the catalyst in the feed line of the SI engine, for various  $NGR/O_2$  ratios and catalysts.

### 3. RESULTS AND DISCUSSION

#### 3.1 Catalyst performance in AGRC

204 The first results presented concern exclusively the catalyst performance when Air Gas Reforming Circulation  
205 (AGRC) is used. All results are given on dry basis. Natural gas and air react chemically over the catalyst; N<sub>2</sub>  
206 is the constituent with the highest concentration at the catalyst input and output. We provide results for H<sub>2</sub>,  
207 CO and unconverted natural gas. To avoid H<sub>2</sub> auto-ignition, as explained previously, the experiment is  
208 designed to ensure there is no O<sub>2</sub> at the catalyst output. The CO<sub>2</sub> concentration is around of 6-7% at the  
209 catalyst output.

210  
211 The primary gases at the exit of the catalyst are shown in Figure 6. In the top two graphs of Figure 6, H<sub>2</sub>  
212 production is seen to depend on the catalyst formulation, and to result in hydrogen concentrations of  
213 approximately 26% for the Pd catalyst and 21% for Pt. H<sub>2</sub> production also depends on the air flow rate,  
214 indicating that fluid dynamic effects are very significant. In the configuration with reformed exhaust gas  
215 recirculation (denoted RGR), where exhaust gas is blended with additional natural gas before entering the  
216 reformer, Le Corre et al. [1] have shown that H<sub>2</sub> production yields a concentration in the reformed gas of only  
217 10-14%. The AGRC improves significantly H<sub>2</sub> production by promoting the partial oxidation of methane, at  
218 temperatures around 775 K. This temperature is not the most favorable for H<sub>2</sub> production (the ideal  
219 temperature for H<sub>2</sub> production is around 1000 K); but the exhaust gases exiting the turbocharger are  
220 available at 775 K for use and are otherwise emitted as wastes.

221  
222 In Figure 6 (middle two graphs), CO production is observed to be significant, leading to a CO concentration  
223 of around 11% for the Pd catalyst and 8% for Pt. Such amounts are not a major problem in IC engines,  
224 contrary to fuel cell applications. As for H<sub>2</sub> production, CO production also depends on the air flow rate,  
225 indicating that fluid dynamic effects are very significant, as is the chemical pathway, denoted by equations 1-  
226 6, over the catalyst.

227  
228 In Figure 6 (bottom two graphs), the concentration of unconverted natural gas content is shown,  
229 demonstrating that O<sub>2</sub> (from additional air) is totally consumed, avoiding the risk of H<sub>2</sub> auto-ignition. When  
230 the additional air flow rate is 3 Nm<sup>3</sup>/h, the experimental facilities are not capable of measuring a NGR/O<sub>2</sub> ratio  
231 lower than 0.3. Clearly, however, the unconverted natural gas concentration is more important at an  
232 additional air flow rate of 3 Nm<sup>3</sup>/h than 5 Nm<sup>3</sup>/h.

233  
234 Figure 7 illustrates the variation in H<sub>2</sub> concentration with CO concentration for the two catalysts and two air  
235 flow rates, and shows the role of catalyst composition (Pd and Pt). In Figure 5, ratios of reformed exhaust  
236 gas recirculation (NGR) to O<sub>2</sub> ranging between 0.3 and 1.6 are considered for the two air flow rates and the  
237 two catalysts. The concentrations of H<sub>2</sub> and CO, respectively, depend on air flow rate, achieving values over  
238 the Pd catalyst of about 26% and 11% at an air flow rate of 3 Nm<sup>3</sup>/h and 20% and 8% at an air flow rate of 5  
239 Nm<sup>3</sup>/h. But H<sub>2</sub> and CO concentrations are not too sensitive to the ratio NGR/O<sub>2</sub> for an air flow rate of 3  
240 Nm<sup>3</sup>/h. Conversely, over the Pt and Pd catalysts, the H<sub>2</sub> and CO concentrations increase approximately  
241 linearly with the NGR/O<sub>2</sub> ratio. This observation suggests that chemical pathway is dependent on the catalyst  
242 choice.

243

244



245 Fig. 6. Variations in concentrations of main gases with the ratio  $\text{NGR}/\text{O}_2$  of at the exhaust of catalyst for two  
246 catalysts and air flow rates.

247

248

249

250 Fig. 7. Variation of  $\text{H}_2$  concentration with  $\text{CO}$  concentration for two catalysts and air flow rates.

251

### 252 3.2 Effects of catalysts on CHP system

253

254 The basic system (the CHP plant) has two inputs: natural gas and air in the main stream. The modified  
255 system (the CHP plant equipped with a catalyst device) is similar, except that the one natural gas stream is  
256 separated in two lines: one to the engine and the other to the catalyst. The absolute difference in electric  
257 efficiency is defined as the difference between the electric efficiencies of the modified and basic systems,  
258 with a positive absolute difference meaning that the catalyst device increases the electric efficiency and a  
259 negative value meaning that the catalyst device decreases the electric efficiency.

260

261 In Figure 8, the variation in the absolute difference of CHP electric efficiency with the ratio  $\text{NGR}/\text{O}_2$  is shown  
262 for both Pd and Pt catalysts and for two air flow rates. In the left graph of Figure 8 for which the additional air  
263 flow rate is  $3 \text{ Nm}^3/\text{h}$ , the absolute difference is positive when the  $\text{NGR}/\text{O}_2$  ratio is less than 1.3. In that figure,  
264 values for Pd (dotted spline line) and Pt (solid spline line) catalysts are seen to improve electric efficiency by  
265 similar amounts. In the left graph of Figure 8 for which the additional air flow rate is  $5 \text{ Nm}^3/\text{h}$ , the absolute  
266 difference of electric efficiency is approximately zero for low values of the ratio  $\text{NGR}/\text{O}_2$  ( $< 0.8$ ) and negative  
267 for high values of that ratio ( $> 0.8$ ). Note that the results in Figure 8 and the related observations correspond  
268 with  $\text{H}_2$  production concentrations of 26% at  $3 \text{ Nm}^3/\text{h}$  and of 20% at  $5 \text{ Nm}^3/\text{h}$ .

269

270 The benefit in electrical efficiency is directly attributable to the ability of  $\text{H}_2$  to promote the combustion  
271 process. Several benefits of hydrogen combustion are described by Bauer and Forest [11]:

- 272 ■ The laminar flame speed for a stoichiometric hydrogen/air mixture (2.65-3.25 m/s) is about seven  
273 times higher than for methane or gasoline in air. This property of hydrogen leads to decreases the  
274 wall heat transfer to 17-25% of the primary fuel energy for hydrogen, compared to 22-33% for  
275 natural gas or 30-42% for gasoline.
- 276 ■ The “quenching distance” defined as the distance from the cylinder wall at which the flame quenches  
277 due to heat losses, characterizes the flame quenching property of a fuel in internal combustion  
278 engines. The quenching distance of hydrogen (0.064 cm at standard conditions) is approximately  
279 three times lower than that of other fuels, such as gasoline (0.2 cm at standard conditions) or  
280 methane (0.203 cm at standard conditions).
- 281 ■ Emissions from hydrogen fuelled engines are neither toxic nor photochemically reactive.

282

283

284

285

286

Fig. 8. Absolute difference of electric efficiency.

287 The uncertainty in the determined electric efficiency for the basic system (when there is no flow over the  
 288 catalyst) is obtained by noting that the electric power  $W_e$ , the low heating value  $LHV$  and the mass flow rate  
 289 of natural gas  $q_{NG}$  are three independent measures (measured by a wattmeter, a gas chromatograph and a  
 290 mass flow meter, respectively):

$$292 \quad d\eta_e = \frac{1}{LHV q_{NG}} dW_e - \frac{W_e}{LHV^2 q_{NG}} dLHV - \frac{W_e}{LHV q_{NG}^2} dq_{NG} \quad (9)$$

293 The quadratic uncertainty  $u(\eta_e)$  is defined based on the uncertainties of these three variables with its norm:

$$295 \quad u(\eta_e)^2 = \left( \frac{1}{LHV q_{NG}} u(W_e) \right)^2 + \left( \frac{W_e}{LHV^2 q_{NG}} u(LHV) \right)^2 + \left( \frac{W_e}{LHV q_{NG}^2} u(q_{NG}) \right)^2 \quad (10)$$

$$297 \quad \left( \frac{u(\eta_e)}{\eta_e} \right)^2 = \left( \frac{u(W_e)}{W_e} \right)^2 + \left( \frac{u(LHV)}{LHV} \right)^2 + \left( \frac{u(q_{NG})}{q_{NG}} \right)^2 \quad (11)$$

298 This is the classical law of uncertainty propagation see [12]. Substituting numerical values shows that the  
 299 relative uncertainty of efficiency  $\frac{u(\eta_e)}{\eta_e}$  is about 2.5%, with  $u(W_e)/W_e = 2\%$ ,  $u(LHV)/LHV = 1\%$  and

301  $u(q_{NG})/q_{NG} = 1\%$ . So the value of the electric efficiency  $\eta_e$  is  $35\% \pm 1.0\%$ .

302 In this investigation, the main instrumentation is shared between the basic system and the modified system  
 303 (wattmeter, gas chromatograph for natural gas, and mass flow meter for natural gas in the main stream).  
 304 The only difference is a second mass flow meter for the additional natural gas entering the catalyst. The  
 305 uncertainty between these two configurations is evaluated, denoting the electric efficiency  $\eta_e^0$  in the basic  
 306 configuration and  $\eta_e^{NGR}$  when the catalyst device is active. The difference  $(\eta_e^{NGR} - \eta_e^0)$  has been measured  
 307 to be about 0.2%, which is equivalent to stating that the ratio  $\frac{\eta_e^0}{\eta_e^{NGR}} \approx 0.99 < 1$ . Here,

$$310 \quad \frac{\eta_e^0}{\eta_e^{NGR}} = \frac{\frac{W_e}{LHV q_{NG_0}}}{\frac{W_e}{LHV (q_{NG_1} + q_{NGR})}} \quad (12)$$

311 Where  $q_{NG_0}$  is the mass flow rate of natural gas in the basic configuration required to produce the electric  
 312 power  $W_e$ , and  $q_{NG_1}$  is the mass flow rate of natural gas in the main stream of the modified configuration.

314 Rearranging this equation yields

315

$$316 \quad \frac{\eta_e^0}{\eta_e^{NGR}} = \frac{q_{NG_1} + q_{NGR}}{q_{NG_0}} \quad (13)$$

317

318 where  $q_{NG_0}$  and  $q_{NG_1}$  are measured by the same mass flow meter. As previously, the ratio  $\frac{\eta_e^0}{\eta_e^{NGR}}$  is

319 obtained by two independent measurements:

$$320 \quad d\left(\frac{\eta_e^0}{\eta_e^{NGR}}\right) = \frac{q_{NG_0} dq_{NG_1} - q_{NG_1} dq_{NG_0}}{q_{NG_0}^2} + \frac{q_{NG_0} dq_{NGR} - q_{NGR} dq_{NG_0}}{q_{NG_0}^2} \quad (14)$$

321 The fact that only one gas flow meter is used in the main stream implies that  $dq_{NG_0} = dq_{NG_1} = dq_{NG}$ . Thus,

$$322 \quad d\left(\frac{\eta_e^0}{\eta_e^{NGR}}\right) = \frac{q_{NG_0} - q_{NG_1}}{q_{NG_0}^2} dq_{NG} + \frac{q_{NG_0} dq_{NGR} - q_{NGR} dq_{NG}}{q_{NG_0}^2} \quad (15)$$

323 and its uncertainty is given by its norm:

$$324 \quad u\left(\frac{\eta_e^0}{\eta_e^{NGR}}\right)^2 = \left(\frac{q_{NG_0} - q_{NG_1} - q_{NGR}}{q_{NG_0}^2} u(q_{NG})\right)^2 + \left(\frac{1}{q_{NG_0}} u(q_{NGR})\right)^2 \quad (16)$$

325

326 Substituting numerical values gives  $u\left(\frac{\eta_e^0}{\eta_e^{NGR}}\right) = 5.04E-4$ . That means that the difference  $(\eta_e^{NGR} - \eta_e^0)$  has an

327 uncertainty of about  $2.0E-4$  and this difference is  $0.2\% \pm 2.0E-4$ .

328

329 A time recording of electric efficiency and H<sub>2</sub> content is plotted on Figure 9 for the following conditions: spark  
330 timing advance 14CA BTDC, 7% O<sub>2</sub> content in the exhaust gases, 80% full load, ambient temperature 21 °C  
331 and relative humidity around 21%. Two gaps exist around 100 s and 1450 s. The first corresponds to turning  
332 off the additional natural gas flow, and the second one to turning it on. It is clear that uncertainties in the  
333 wattmeter or the gas chromatograph are not notable. Only the uncertainties of the two mass flow meters are  
334 important, as seen in equation 15.

335

336 Fig. 9. Time recording of electric efficiency and H<sub>2</sub> production.

337

338

339 An increase of electric efficiency is beneficial, but may not be acceptable if it increases exhaust gases  
340 emissions. In Figure 10, the variation in CO and HC emission concentrations in exhaust line of the CHP  
341 plant with the ratio NGR/O<sub>2</sub> are shown for the Pd catalyst and two air flow rates. It can be seen in the figure  
342 that the effect of the catalyst device is not significant on CO and HC emission concentrations, regardless of  
343 the additional air flow rate and the ratio NGR/O<sub>2</sub>. Thus the increase of electric efficiency with the catalyst  
344 device does not appear to come at the expense of increased emissions, so a retrofit to achieve the absolute  
345 difference of electric efficiency is worth considering.

346

347

348 Fig. 10. Variation with NGR/O<sub>2</sub> ratio of the exhaust emission concentrations of the CHP plant equipped with  
349 a Pd catalyst device, for two air flow rates.

### 350 3.3 Discussion

351 Several processes used to improve the performance of engines are compared in Table 3. In this table, an SI  
352 engine fuelled by natural gas under lean conditions (taken to be an equivalence ratio of 1.4) equipped with a  
353 two-way catalyst (CO and unburned hydrocarbon UHCs oxidations) in the exhaust line is referred to as the  
354 Base case. Exhaust emissions of UHC, CO are considered after the two-way catalyst in the exhaust line.  
355 The modified engine cases considered include the Base case with exhaust gas recirculation (EGR), the  
356 Base case with reformed gas recirculation (RGR), and the Base case with air gas reforming circulation  
357 (AGRC). It is seen that the use of EGR and RGR processes improves engine environmental performance  
358 (especially NO<sub>x</sub> emissions) but lowers energetic performance in terms of efficiency. However, the application  
359 of the AGRC concept to the GUASCOR engine increases the energy efficiency of the engine by around 0.2-  
360 0.4%, with little change in environmental performance. The results in Table 3 need to be validated on other  
361 types of engines having different control loops.

362

363

364 Table 3. Comparison of impact on technical and environmental performance of various engine modifications  
365 relative to a base case engine.

366

### 367 3.4 Engine knock issues and resolutions

368

369 The main risk of adding H<sub>2</sub> in internal combustion engines is the occurrence of knock associated with  
370 abnormal combustion. IC engines used for CHP installations usually run under strict operating conditions,  
371 usually based on achieving maximum electricity output while maintaining emissions at acceptable levels, as  
372 outlined in the Introduction. Hydrogen addition to natural gas decreases its relative methane content and is  
373 known to increase its ability to detonate. Hence, the knock tendency of an engine must be closely monitored  
374 when adding H<sub>2</sub> to increase engine efficiency.

375

376 Knock, which has been a concern since the invention of the IC engine, is caused by a local auto-ignition of  
377 gases under specific thermodynamic conditions, can seriously damage an engine (see Figure 11).  
378 Consequently, design and operating conditions are often limited by knock conditions.

379

380

381 Fig. 11. Piston damage from engine knock.

382

383

384 For knock problems, the methane number *MN* is commonly used to represent the gas quality, i.e. its ability  
385 to resist auto-ignition. It is usually equal to 100 for pure methane and 0 for pure hydrogen. This indicator is  
386 the equivalent of the Research Octane Number (*RON*) used for liquid fuels such as gasoline.

387

388 SI engines used as CHP plant can produce more than 1 MWe. Then, it is better to conceive a preventive  
389 protection instead of a curative one, as described by Le Corre et al. [13] and Saikaly et al. [14-16]. This is

390 especially true for applications involving hydrogen, where it is more advantageous to avoid knock rather than  
391 to detect it.

392

393 Knock conditions can be avoided by using AGRC, not to maximize the electric production but to protect the  
394 engine. Note that the methane number of reformed gas is calculated on the same basis as for natural gas,  
395 i.e., without inert gases. Since natural gas and reformed gas have two different methane numbers, it is  
396 possible to adjust the setting for the CHP plant to avoid knock conditions. This approach can form the basis  
397 of a preventive control mechanism.

398

399 A recent patent (number WO 2011010069) by Rahmouni and Le Corre [17] aims to avoid the occurrence of  
400 knock by using two methane number sensors (labeled 21 and 50 in Figure 1) to control the natural gas flow  
401 rates (both the main stream and the additional stream) to maintain an acceptable value entering the SI  
402 engine. These sensors are described in detail by Rahmouni et al. [18-20] and Loubar et al. [21].

403

404

405 Table 4. Methane number of natural gas and reformed gas

406

#### 407 **4. CONCLUSIONS**

408

409 In this paper, air gas reforming circulation (AGRC) is proposed as a solution for in situ H<sub>2</sub> production for  
410 spark ignition engines fuelled by natural gas. Several important conclusions can be drawn from the results:

411

412 • With AGRC, the concentrations of the constituents of the reformed gas are approximately 25%  
413 H<sub>2</sub>, 10% CO, 8% unburned hydrocarbons and 55% N<sub>2</sub>. The AGRC reformed gas is blended with  
414 the main flow of natural gas and air, so unconverted natural gas is mixed with natural gas and is  
415 not problematic. The low heating value of CO is counterbalanced by the effect of H<sub>2</sub> during  
416 combustion in the cylinder of SI engine.

417 • The overall electric efficiency of an engine increases by 0.2% when the AGRC system is  
418 applied. Although the increase is not large, it is balanced by the fact that the AGRC system is  
419 simple to setup and cost effective.

420 • Equipping an SI engine with AGRC does not change significantly exhaust emissions (CO and  
421 HC) in comparison with the original configuration.

422 • AGRC appears to be advantageous compared to reformed gas recirculation because RGR  
423 decreases the electric efficiency of the overall system compared to an SI engine without  
424 reforming, while AGRC improves the electric efficiency.

425 • No knock or misfiring occurred during experimental tests. But, if abnormal conditions appear for  
426 some operating conditions, it is possible to adjust the natural gas main flow and the AGRC flow  
427 to avoid the problematic conditions by measuring and controlling the relative methane content  
428 of the combustion mixture so that it remains in the correct operating window, as defined by the  
429 engine manufacturer.

430

431 **ACKNOWLEDGEMENTS**

432 Authors would like to thank Dr C. Rahmouni, Dr S. Rousseau and Dr L. Truffet for their valuable  
433 contributions.

434

435 **REFERENCES**

- 436 [1] Le Corre O., Rahmouni C., Saikaly K. and Dincer I. (2011), Effect of H<sub>2</sub> produced through steam methane  
437 reforming on CHP plant efficiency, *International Journal of Hydrogen Energy*, 36(17):11457-11466.
- 438 [2] Einewall P., Tunestal P. and Johansson B. (2005), Lean burn natural gas operation vs. stoichiometric  
439 operation with EGR and a three way catalyst, *Society of Automotive Engineers*, paper 2005-01-0250.
- 440 [3] Yap D., Peucheret S.M., Megaritis A., Wyszynski M.L. and Xu H. (2006), Natural gas HCCI engine  
441 operation with exhaust gas fuel reforming. *Int. J. Hydrogen Energy*, 31(5):587-595.
- 442 [4] Hadj-Sadok Ouaguenouni M., Benadda A., Kiennemann A. and Barama A. (2009), Preparation and  
443 catalytic activity of nickel-manganese oxide catalyst in the reaction of partial oxidation of methane, *Comptes*  
444 *Rendus Chimie*, 12(6-7):740-747.
- 445 [5] Torniainen P.M., Chu X. and Schmidt L.D. (1994), Comparison of monolith-supported metals for the  
446 direct oxidation of methane to syngas, *J. Catal.* 146(1):1-10.
- 447 [6] Schmidt L.D. and Huff M. (1994), Partial oxidation of CH<sub>4</sub> and C<sub>2</sub>H<sub>6</sub> over noble metalcoated monoliths,  
448 *Catalysis Today*, 21(2-3):443-454.
- 449 [7] Schmidt L.D., Deutschmann O. and Goralski Jr. C.T. (1998), Modeling the partial oxidation of methane to  
450 syngas at millisecond contact times, *Studies in Surface Science and Catalysis*, 119:685-692.
- 451 [8] Deutschmann O. and Schmidt L.D. (1998), Modeling the partial oxidation of methane in a short-contact-  
452 time reactor, *AIChE Journal*, 44(11):2465-2477.
- 453 [9] Le Corre O., Rousseau S. and Sollicec C. (1998), One zone thermodynamic model simulation of a  
454 stationary spark ignition gas engine: Static and dynamic performances, *Society of Automotive Engineers*,  
455 paper 982694.
- 456 [10] Peucheret S., Wyszynski M.L., Lehrle R.S., Golunski S. and Xu H. (2005), Use of catalytic reforming to  
457 aid natural gas HCCI combustion in engines: experimental and modelling results of open-loop fuel,  
458 *International Journal of Hydrogen Energy*, 30(15):1583-1594.
- 459 [11] Bauer C.G., Forest T.W (2001), Effect of hydrogen addition on the performance of methane-fueled  
460 vehicles. Part I: Effect on S.I. engine performance, *International Journal of Hydrogen Energy*, 26(1):55-70.
- 461 [12] ISO/IEC Guide 98-3:2008 Guide to the expression of uncertainty in measurement (GUM). *International*  
462 *Organization for Standardization*.
- 463 [13] Le Corre O., Rahmouni C., Rousseau S. and Truffet L. (2008), Method for protecting a gas engine and  
464 associated device. Patent WO2008035014, 27 March 2008.
- 465 [14] Saikaly K., Rousseau S., Rahmouni C. and Le Corre O. (2008), Safe operating conditions determination  
466 for stationary SI gas engines, *Fuel Processing Technology*, 89(11):1169-1179.
- 467 [15] Saikaly K., Le Corre O. and Rahmouni C. (2010), Preventive knock protection technique for stationary  
468 SI engines fuelled by natural gas, *Fuel Processing Technology*, 91(6):641-652.
- 469 [16] Saikaly K., Rahmouni C., Le Corre O. and Truffet L. (2009), Industrial application of a preventive knock  
470 technique, *Society of Automotive Engineers*, paper 2009-01-2750.
- 471 [17] Rahmouni C. and Le Corre O. (2010), Reforming method, and energy conversion machine including  
472 reforming device. Patent WO2011010069, 27 Jan. 2011.

- 473 [18] Rahmouni C., Tazerout M. and Le Corre O. (2003), Method for determining at least one energetic  
474 property of a gas fuel mixture by measuring physical properties of the gas mixture. Patent WO03012435, 28  
475 April 2004.
- 476 [19] Rahmouni C., Tazerout M. and Le Corre O. (2003), Determination of the combustion properties of  
477 natural gases by pseudo-constituents, *Fuel*, 82(11):1399-1409.
- 478 [20] Rhamouni C., Le Corre O. and Tazerout M. (2003), Online determination of natural gas properties,  
479 *Comptes Rendus Mécanique*, 331(8):545-550.
- 480 [21] Loubar K., Rahmouni C., Le Corre O. and Tazerout M. (2007), A combustionless determination method  
481 for combustion properties of natural gases, *Fuel*, 86(16):2535-2544.
- 482 [22] Leiker M., Cartelliere W., Christoph H., Pfeifer U. and Rankl M. (1972), Evaluation of antiknocking  
483 property of gaseous fuels by means of methane number and its practical application to gas engines, *Diesel  
484 & Gas Engine Power Conference & Exhibition*, American Society of Mechanical Engineers, St. Louis, Mo.,  
485 Paper No. 72-DGP-4, pp. 1-16.
- 486
- 487

## List of figures

- 488  
489  
490 Fig. 1. Variation of selected engine performance parameters with equivalence ratio, highlighting challenges  
491 (firing problems, emissions) in improving engine performance
- 492  
493 Fig. 2. Engine system incorporating the air gas reforming circulation (AGRC) concept.
- 494  
495 Fig. 3. Reforming device installation (at left) on a 210 kW<sub>e</sub> CHP gas engine (orange).  
496 *Legend: (10) air flow meter, (11) air filter, (12) carburetor, (13) turbocharger, (14) intercooler, (15) actuator,*  
497 *(16) engine, (17) catalyst device, (18) exhaust heat exchanger, (20) natural gas flow meter, (21) Methane*  
498 *Number sensor, (30) additional air flow meter, (40) additional natural gas flow meter, (50) methane number*  
499 *sensor.*
- 500  
501 Fig. 4. Schematic of catalytic device. UHC denotes unburned hydrocarbons.
- 502  
503 Fig. 5. Experimental design of flow rates of additional air over the catalyst in the feed line of the SI engine,  
504 for various NGR/O<sub>2</sub> ratios and catalysts.
- 505  
506 Fig. 6. Variations in concentrations of main gases with the ratio NGR/O<sub>2</sub> of at the exhaust of catalyst for two  
507 catalysts and air flow rates.
- 508  
509 Fig. 7. Variation of H<sub>2</sub> concentration with CO concentration for two catalysts and air flow rates.
- 510  
511 Fig. 8. Absolute difference of electric efficiency.
- 512  
513 [Fig. 9. Time recording of electric efficiency and H<sub>2</sub> production.](#)
- 514  
515 Fig. 10. Variation with NGR/O<sub>2</sub> ratio of the exhaust emission concentrations of the CHP plant equipped with  
516 a Pd catalyst device, for two air flow rates.
- 517  
518 Fig. 11. Piston damage from engine knock.

## List of tables

- 519  
520  
521  
522  
523 Table 1. Engine specifications.
- 524  
525 Table 2. Features of tested catalysts
- 526  
527 Table 3. Comparison of impact on technical and environmental performance of various engine modifications  
528 relative to a base case engine.
- 529  
530 Table 4. Methane number of natural gas and reformed gas
- 531



Table 1. Engine specifications.

Parameter	Value/Description
Engine manufacturer	GUASCOR FGLD 180
Number of cylinders	6
Bore	152 mm
Stroke	165 mm
Displaced volume by cylinder / total	2,994 / 17,964 cm <sup>3</sup>
Clearance volume	300 cm <sup>3</sup>
Compression ratio	11:1
Number of suction valves/exhaust valves	2 / 2 per cylinder
Valve train*: IO/IC/EO/EC	25 CA ATDC/ 45 CA ABDC/ 60 CA BBDC/ 15 CA BTDC
Turbo-charger pressure	1.8 bar
Engine speed	1,500 RPM
Ignition timing	14 CA BTDC

\* CA: crankshaft angle; ATDC: after top dead center; BBDC: before bottom dead center; ABDC: after bottom dead center; BTDC: before top dead center; IO: inlet opens before TDC; IC: inlet closes after BDC; EO: exhaust opens before BDC; EC: exhaust closes after TDC.

Table 2. Features of tested catalysts

Parameter	Value
Catalyst reference code	DC10LQ-1W10-21
Hourly space velocity (HSV)	28,000 h <sup>-1</sup>
Length of honey-comb catalyst	9 cm
Diameter of honey-comb catalyst	21.7 cm

Table 3. Comparison of impact on technical and environmental performance of various engine modifications relative to a base case engine.

Performance parameter	Modified engine cases		
	Base case with EGR	Base case with RGR	Base case with AGRC
Electrical efficiency	Decrease by 2% absolute	Decrease by about 1.5% absolute	Increase by 0.2-0.4% absolute
NOx emissions	Decrease	Same effect as EGR	No important effect
CO emissions	Increase	Same effect as EGR	No important effect
UHC emissions	Increase	Same effect as EGR	Slight decrease
Valve fouling	EGR valve fouling problem	RGR valve fouling problem	No fouling problem (no valve on exhaust line; standard valve on air line)

Table 4. Methane number of natural gas and reformed gas

Content (vol. %)	Natural gas	Reformed gas with AGRC
O <sub>2</sub>	0	0
CO <sub>2</sub>	0.54	6.28
N <sub>2</sub>	2.85	56.25
H <sub>2</sub>	0	21.17
H <sub>2</sub> S	0	0
CO	0	8.14
CH <sub>4</sub>	87.68	8.16
C <sub>2</sub> H <sub>6</sub>	3.04	0
C <sub>3</sub> H <sub>8</sub>	5.6	0
C <sub>4</sub> H <sub>10</sub>	0.29	0
MN*	71.8	78.8

\* Methane number is calculated based on the definition of Leiker et al. [22].

Figure 1

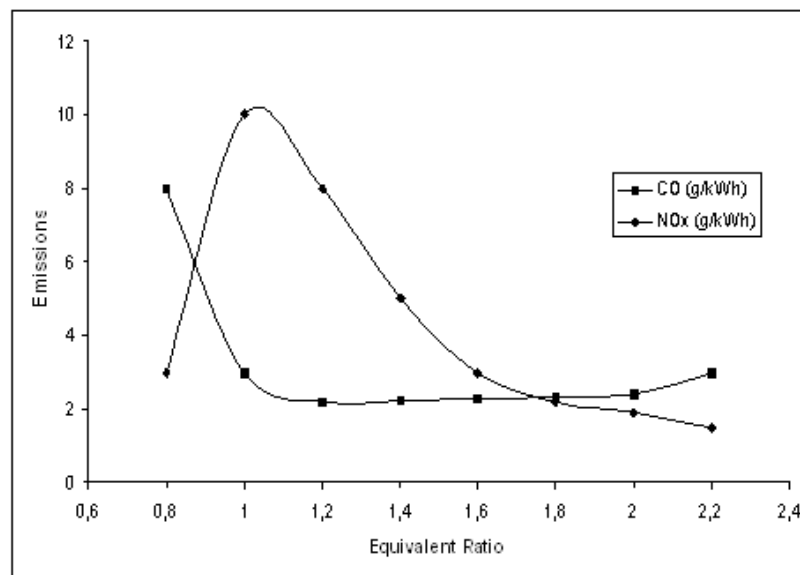
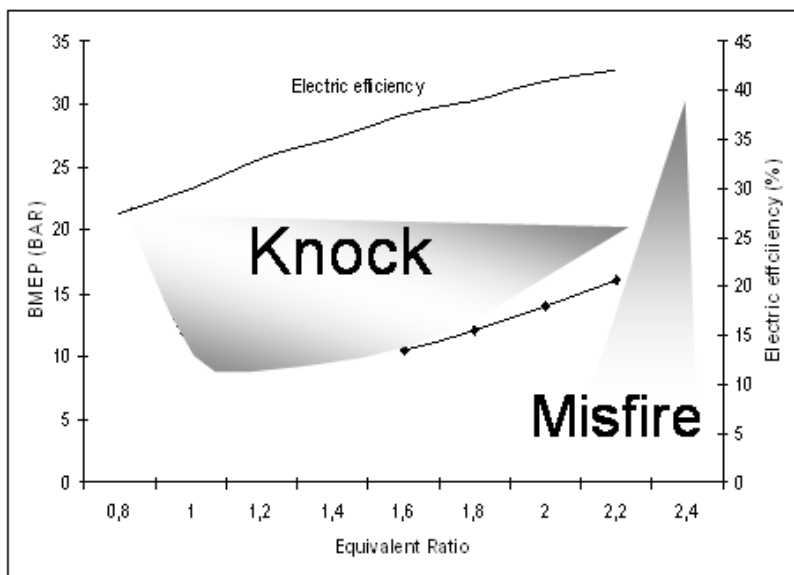


Figure 2

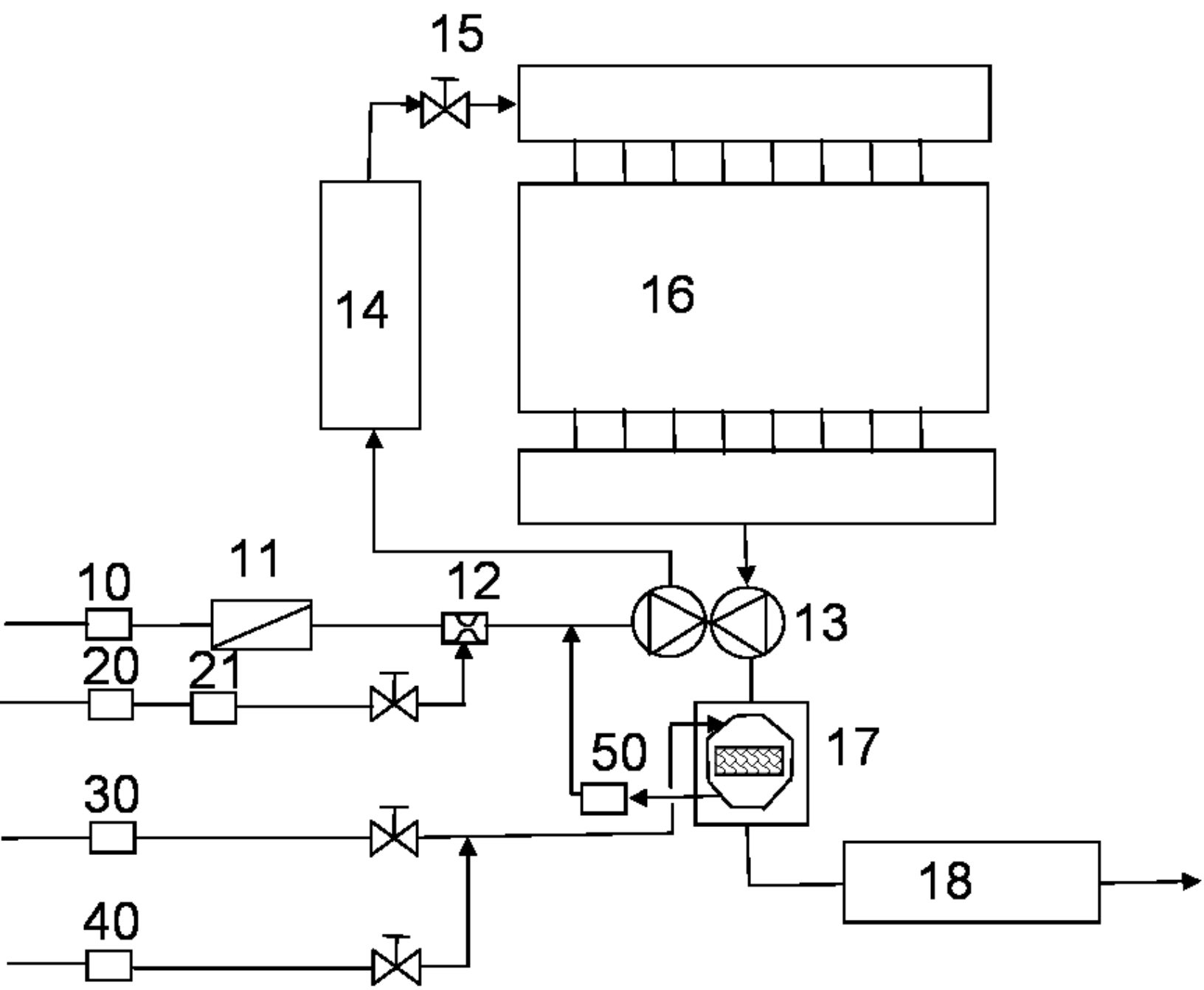


Figure 3



Natural gas  
Main stream

Additional  
natural gas  
towards catalyst device

Figure 4

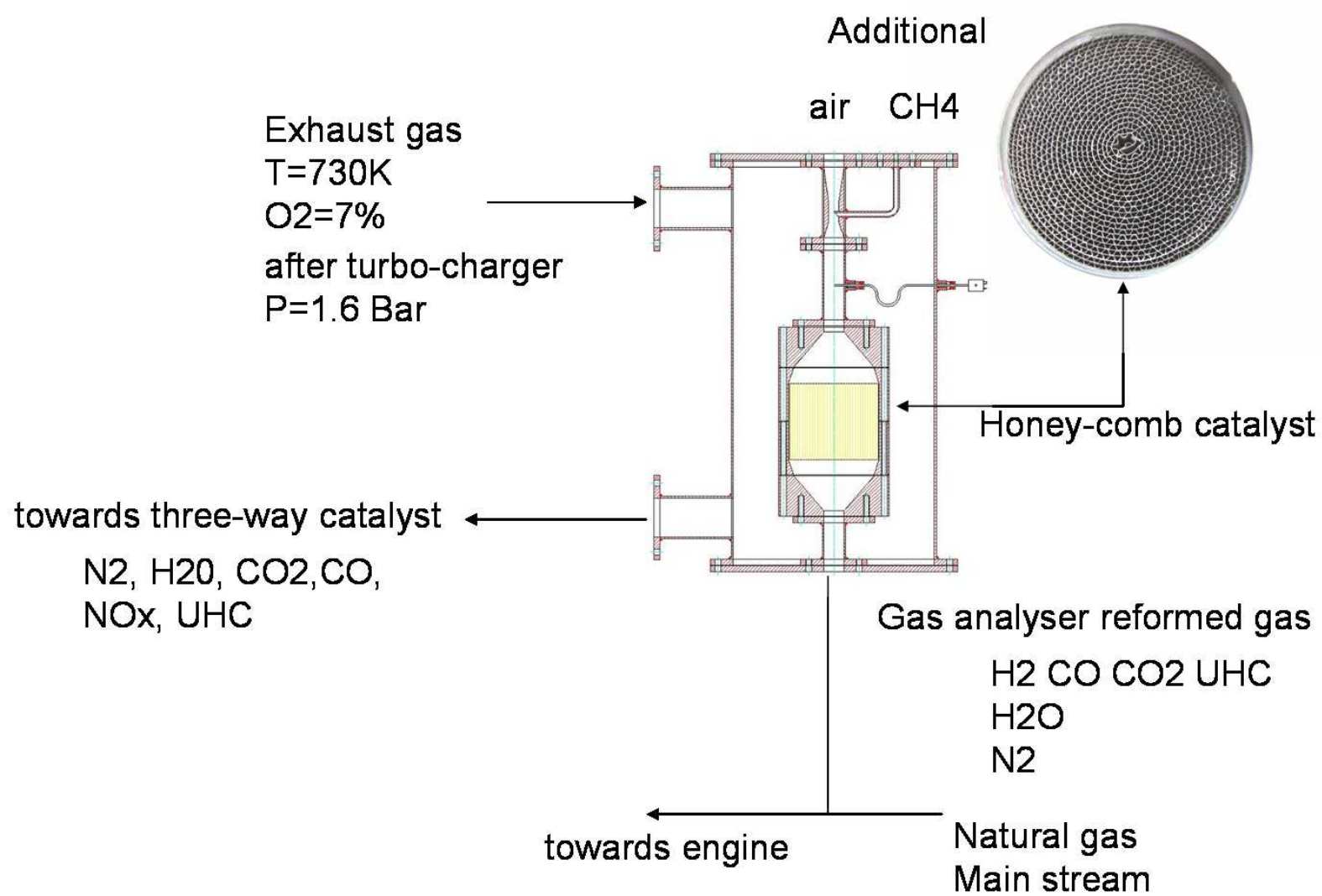




Figure 5

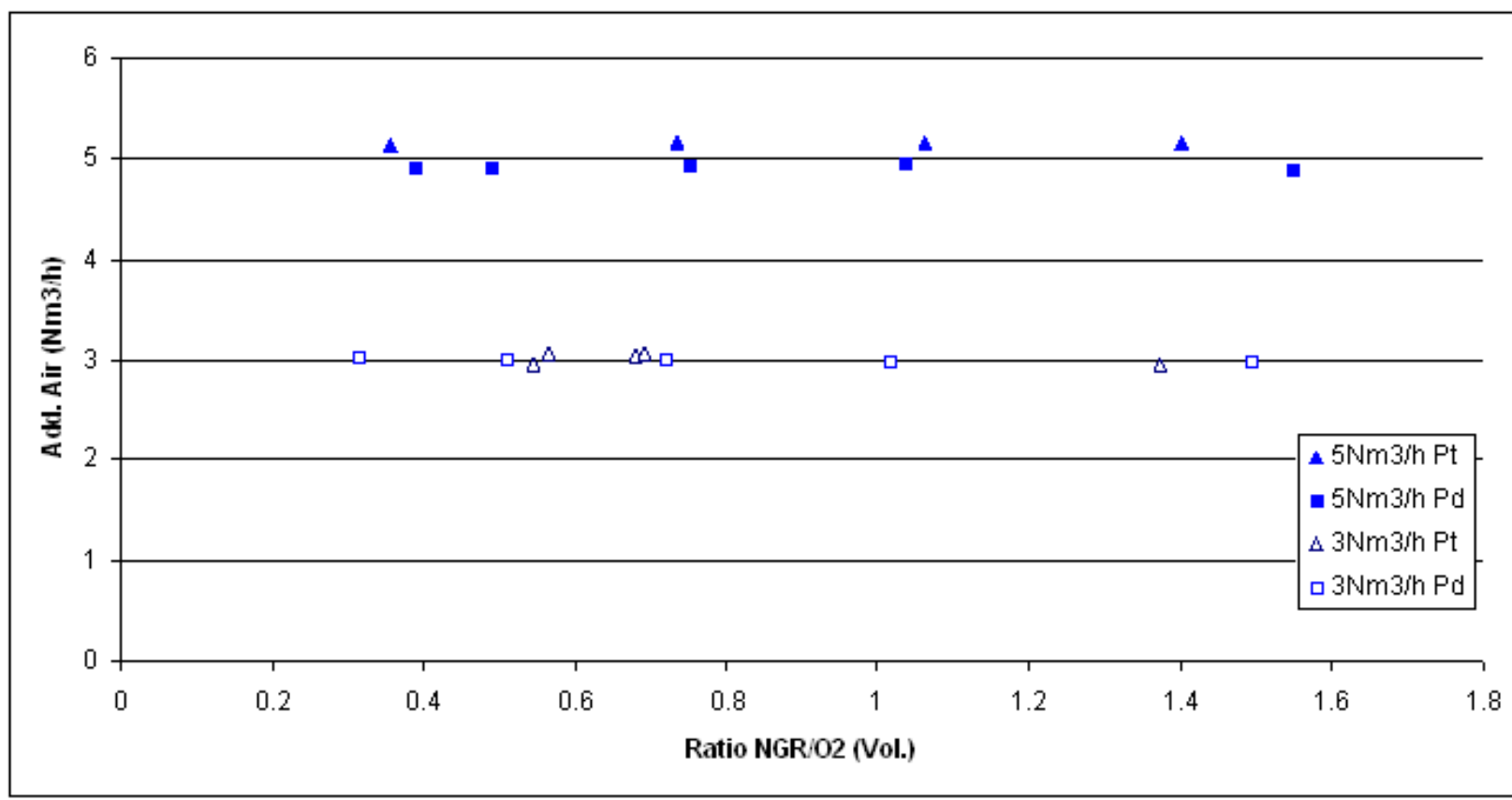


Figure 6

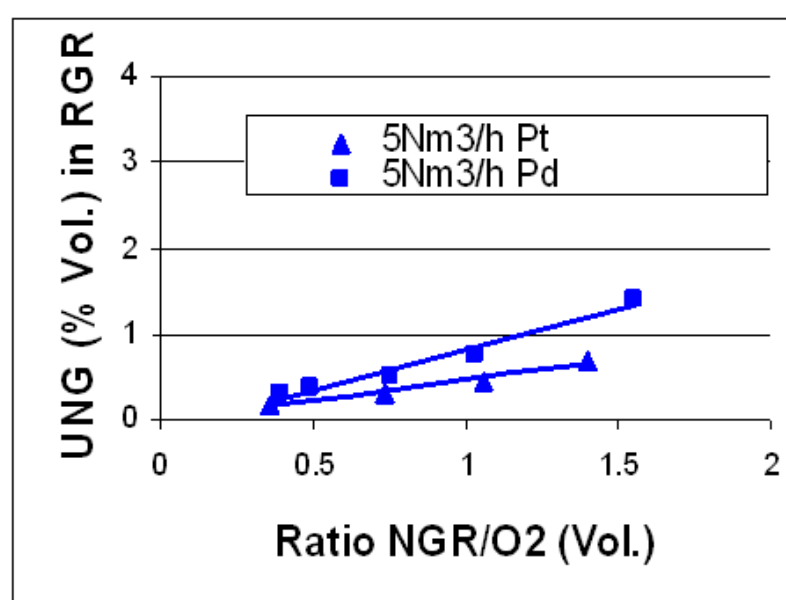
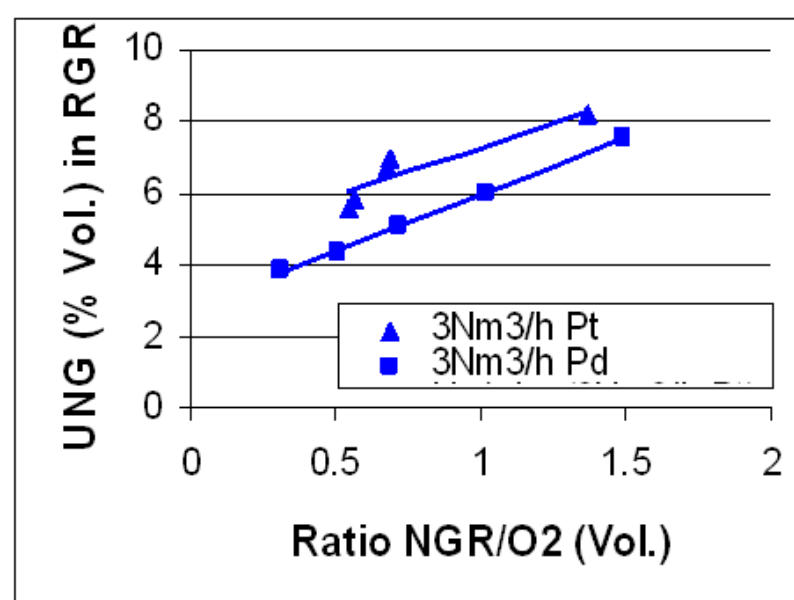
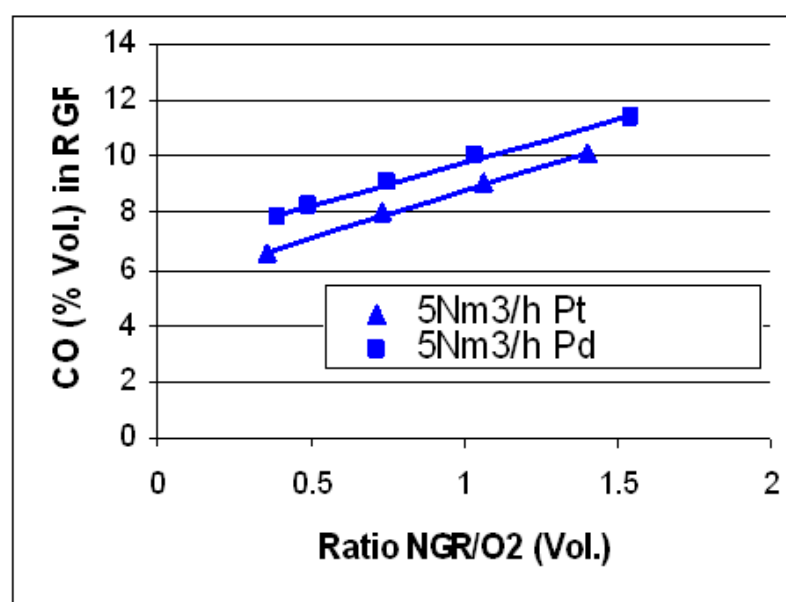
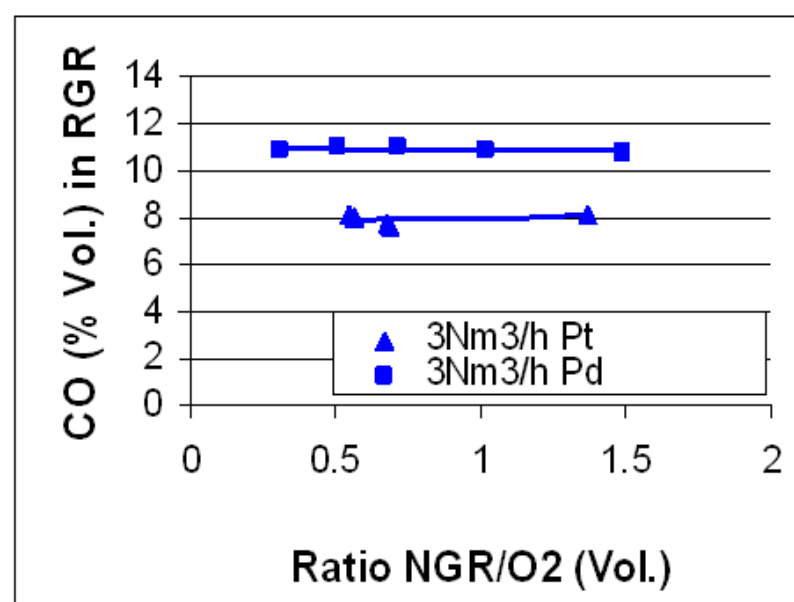
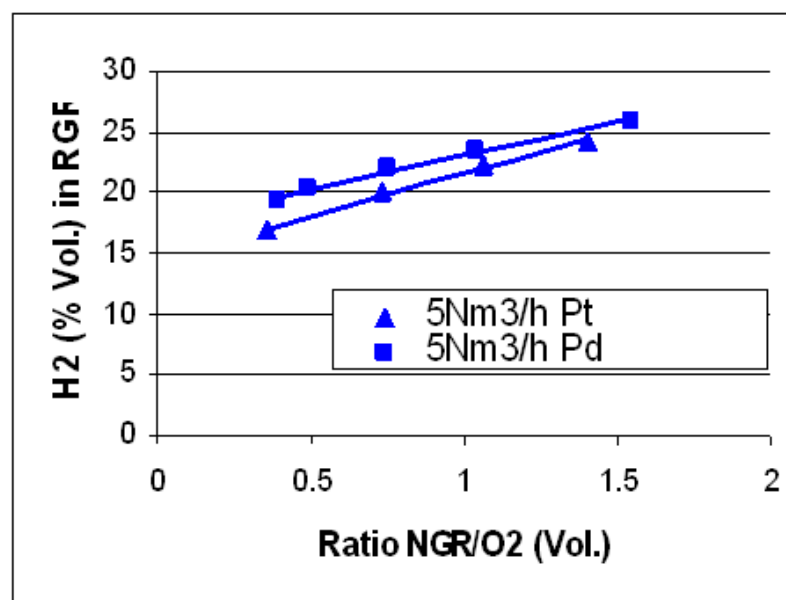
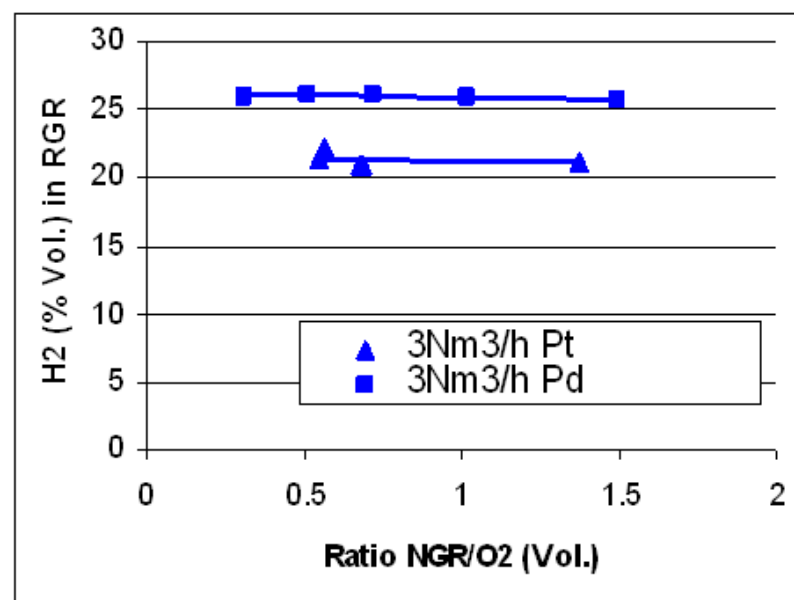


Figure 7

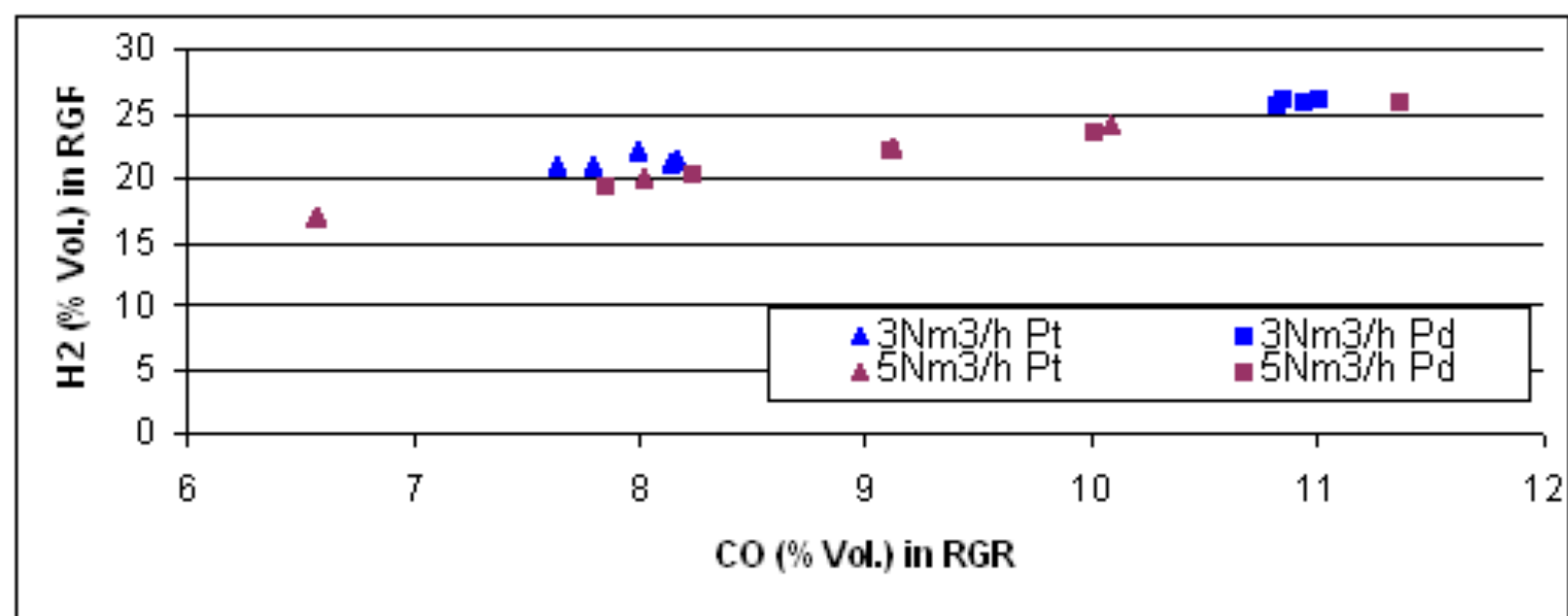


Figure 8

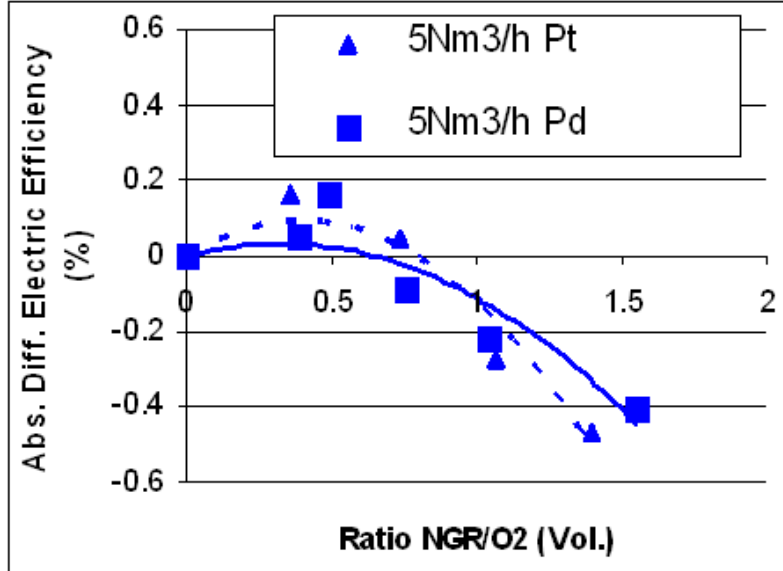
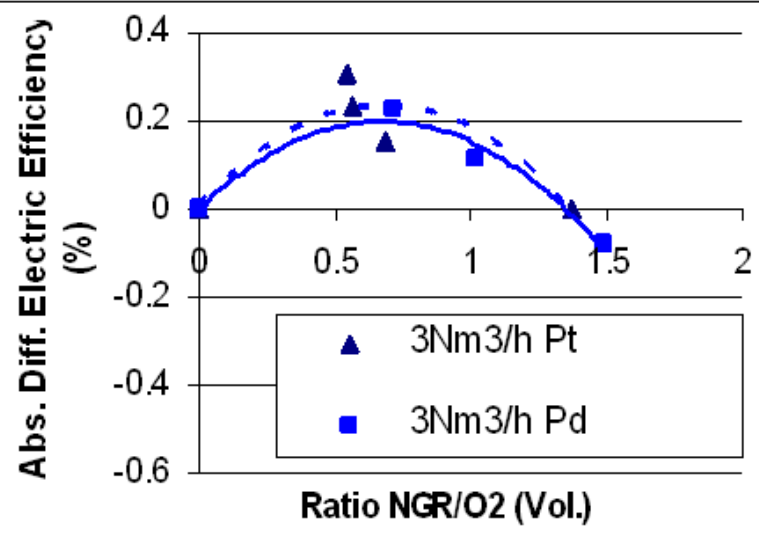


Figure 9

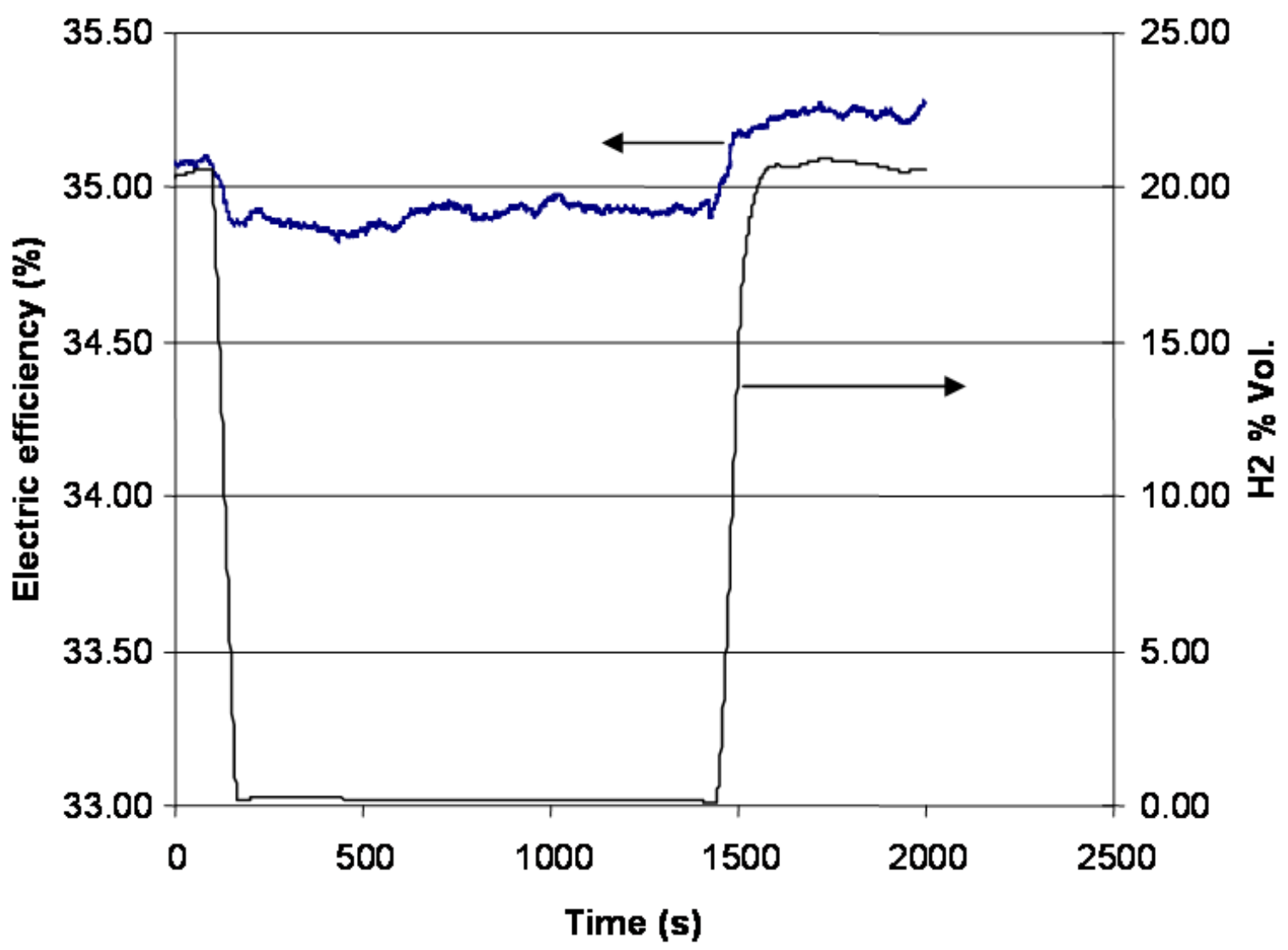


Figure 10

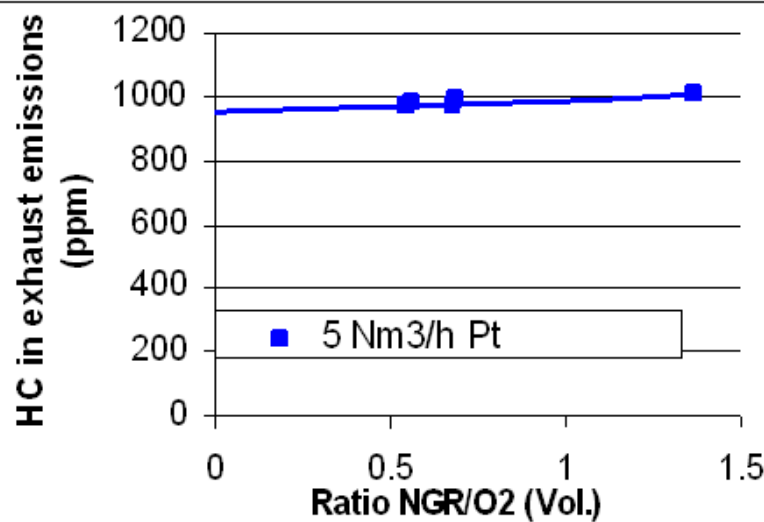
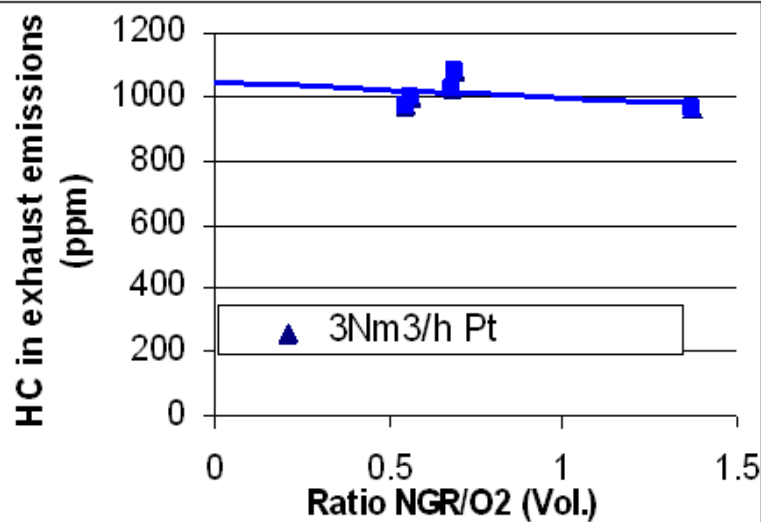
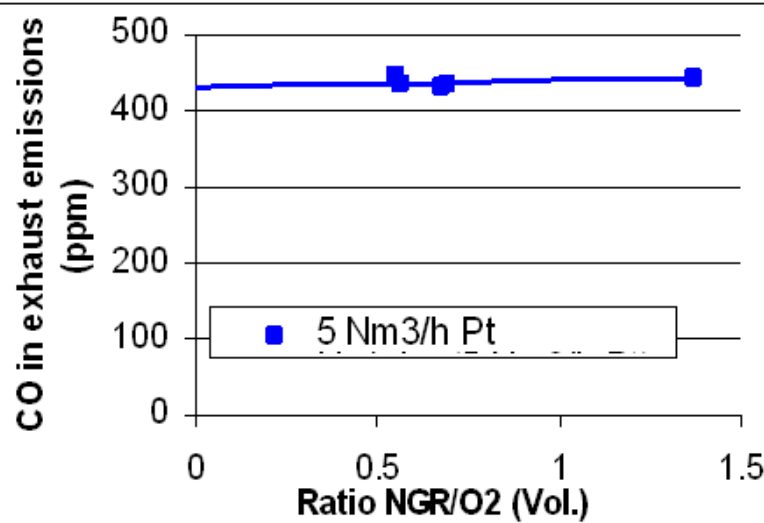
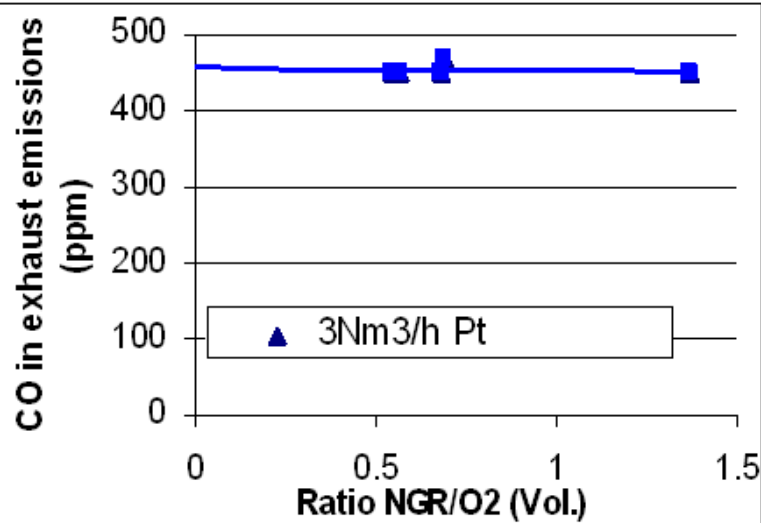


Figure 11

